MINERALOGY AND IRON CONTENT OF THE LUNAR POLAR REGIONS USING THE KAGUYA SPECTRAL PROFILER AND THE LUNAR ORBITER LASER ALTIMETER. M. Lemelin[1], P. G. Lucey[2], K. Jha[3] and D. Trang[2], [1]Department of Earth & Space Science & Engineering, York University, Room 102 Petrie Science and Engineering Building, 4700 Keele St, Toronto, ON, Canada M3J 1P3, lemelin@yorku.ca, [2]Hawaii Institute of Geophysics and Planetology, Department of Geology and Geophysics, University of Hawaii at Manoa, 1680 East-West Rd, POST 602, Honolulu, HI 96822, USA, [3]NASA Goddard/Sigma Space Corporation, 4600 Forbes Boulevard, Lanham, MD 20706, USA.

Introduction: Quantitative assessment of the mineralogical composition of the lunar surface using visible (VIS) and near-infrared (NIR) wavelengths can be obtained by comparing well calibrated reflectance spectra to modeled spectra of known composition, and assigning the composition to the best spectral match using FeO as a constraint [e.g., 1,2]. Due to the low axial tilt of the Moon with respect to the ecliptic, the radiance measured in these wavelengths in the polar regions vary with topography reaching extreme lows in topographic depressions and highs on equator-facing slopes. Calibrated reflectance data including a precise topographic correction has not been derived yet and the available polar FeO abundances (measured by Lunar Prospector) have a spatial resolution of 15 km per pixel. As a result, beside a few local studies [e.g., 3-5], mineral maps have generally been constrained to within 50° in latitude. The mineralogy of the polar regions, which corresponds to more than 16 million km^2 poleward of 50° in latitude, or ~44% of the lunar surface, is mostly unknown.

In this study, we take a novel approach to derive the first mineral and FeO maps of the polar regions (50-90° in latitude) at 1 km per pixel. We take advantage of the newly available calibrated reflectance data from the Lunar Orbiter Laser Altimeter (LOLA) and use it along with reflectance ratio from the Kaguya Spectral Profiler (SP) to derive the first high resolution FeO maps of the polar regions. We use continuum-removed reflectance data acquired by SP during the North and South polar summers and radiative transfer equations to model the mineral abundances of each spectrum, constrained by its abundance in FeO.

Datasets :

LOLA has been actively acquiring reflectance data of the Moon since 2009; it sends a laser pulse towards the Moon at 1064 nm and measures the energy returned from the surface at 0° phase angle, regardless of the Sun's illumination conditions [6]. It provides high signal to noise ratio for the entire lunar surface, regardless of topography, and has been thoroughly calibrated and gridded into polar maps of 1 km per pixel [7].

SP is a spot spectrometer which conducted continuous spectral observations in the visible to near infrared region (500-2600 nm) between 2007 and 2009, with ~550 m spacing between each spectrum [8,9]. Here we used SP data level 2B1, which contains radiometrically calibrated radiance data converted to diffuse reflectance. We applied the photometric function of Yokota et al. [10] to correct for the observational geometry in the 742.8 to 1555.5 nm wavelength range, and obtained the reflectance at an incidence angle of 30° and emission angle of 0°. As this photometric function assumes a flat surface, the resulting reflectance values have important residual errors related to topography, and thus we use reflectance ratios in the derivation of the FeO algorithm, and continuum-removed reflectance in the radiative transfer analysis, as both of these types of data cancel the effects of topography on reflectance. We used data from ~2000 orbits (orbits ~2000-2999, ~4000-4999) which were acquired during the north and south polar summers, in order to maximize the extent of illuminated areas and the strength of the signal [10].

Methods :

We used the 955.5/752.8 nm reflectance ratio from SP and calibrated reflectance at 1064 nm from LOLA to derive polar maps of FeO at 1 km per pixel, using the method of Lucey et al. [11]. To minimize the influence that topography could have on the derivation of the FeO algorithm, we first derived the FeO algorithm in the equatorial region using SP data only (including 1064 nm). We then adapted the algorithm for the polar regions, by replacing the SP reflectance at 1064 by the LOLA reflectance. As LOLA and SP have different viewing geometries, we calculated a scaling factor to be applied to the LOLA data (derived from equatorial measurements of both datasets, far from any topographic effect). We compared the polar FeO abundances derived from SP and LOLA with the abundances measured by the Lunar Propector Gamma-Ray Spectrometer [12] and found them to be in excellent agreement (r = 0.96, σ = 5 wt.%). We calculated the average abundance of FeO in each dataset in 1° latitudinal bins, and found them to be within ~2 wt.% at all latitudes. The largest difference in FeO content between the two datasets occurs near the poles in both polar regions, where the FeO content of SP and LOLA is ~2 wt.% higher than the FeO content of LP. This higher abundance might be due to residual photometric effects in the SP dataset. We performed a latitudinal correction by scaling the SP and LOLA-derived FeO to the LP-derived FeO conent.

To derive quantitative mineral abundances, we compared continuum-removed SP reflectance spectra between 742.8 and 1555.5 nm, to continuum-removed spectra we modeled using radiative transfer equations

(which describe the scattering of light interacting with intimately mixed particles larger than the wavelength). We then assigned a composition to each SP point by searching for the best spectral match, ensuring that the best spectral fit contains within ±5 wt.% FeO of the given SP point. We modeled 6601 mixtures of olivine, low-calcium pyroxene, high-calcium pyroxene and plagioclase. We modeled nine different amount of nanophase iron (0-0.7 wt.% [13]) and Britt-Pieters particles [14], as well as two different grain sizes (17 and 200 μm) for each of these 6601 mineral mixtures. A grain size of 17 μm is optically dominant [15] and a grain size of 200 μm is required to match the observed band depth in plagioclase-rich spectra [3]. We used a fixed Mg-Number of 65. This resulted in 118,818 modeled spectra. We used the optical constants of Lucey [16] optimized to minimize the error between modeled spectra and spectra acquired by the Lunar Soil Characterization Consortium (9 wt.% without the FeO constraint). We did not analyze all the pixels from the ~2000 orbits, as some SP data point have very low signal. We analyzed only the data points that have a signal to noise ratio greater than 20, and radiance greater than 3 W/sr/m^2/nm at 752.8 and 955.4 nm, the wavelengths used in the FeO algorithm. To calculate the signal to noise ratio, we divided the amplitude of the radiance between 746.8 and 1555.5 nm (*i.e.*, the signal), by the standard deviation of the difference in radiance between the odd and even channels (*i.e.*, the noise). This cut-off maximized the number of reflectance measurements while minimizing the noise; this left ~860,000 reflectance measurements in the South polar region, and ~1,200,000 in the North polar region.

Results and conclusion:

Preliminary results show that the FeO and mineral mapping methods are promising. The new FeO abundance maps derived herein at 1 km/pixel resolves details such as pyroclastic deposits (e.g., in Schrödinger basin with ~10-15 wt.% and in J. Herschel crater with ~13-18 wt.%) and some units with high FeO content (e.g., up to ~15-20 wt.% FeO in Mare Frigoris, Mare Humboldtianum, Mare Australe and in the South Pole-Aitken basin). The mineral maps reveal that low-calcium is widely abundant (especially in the South Pole-Aitken with up to ~40 wt.%). High-calcium pyroxene is less abundant (up to ~10 wt.%) and especially concentrated in the center of the South Pole-Aitken basin [5]. We find exposures with ≥98 wt.% plagioclase on the rim of Shackleton crater (Fig. 2) consistent with the observations of Yamamoto et al. [4].

Next, in an effort to reduce the orbit-to-orbit noise resulting from the interpolation of the SP points into mineral maps, we will derive new versions of the mineral maps using data points from the nearly 7000 available SP orbits.

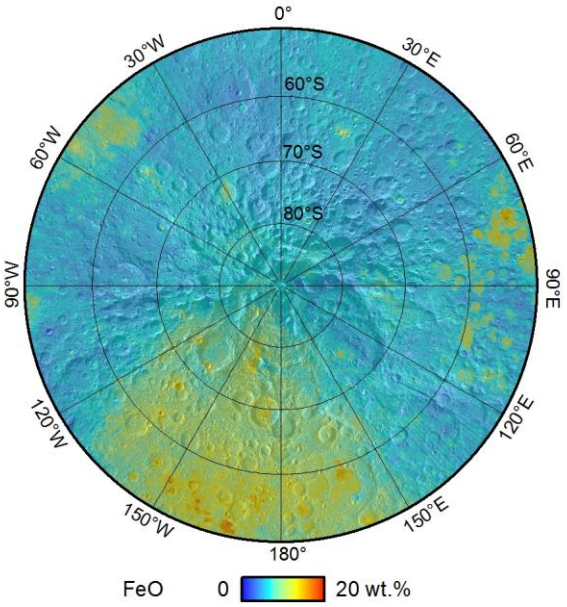

Figure 1. South polar map of FeO derived using Kaguya Spectral Profiler 955.5/752.8 nm, and LOLA 1064 nm reflectance at 1km/pixel.

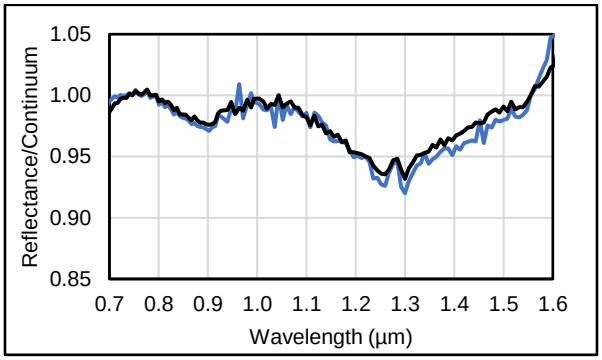

Figure 2. Continuum removed spectra of two exposures with ≥98 wt.% plagioclase on the rim of Shackleton crater detected herein (orbits 4481 and 4482).

References: [1] Lucey P.G. (2004) *GRL, 31*, L08701. [2] Lemelin M. et al. (2015) *JGR, 120*, 869-887. [3] Ohtake M. et al. (2009) *Nature, 461*, 236-241. [4] Yamamoto S. et al. (2012) *GRL, 39(L13201)*. [5] Ohtake M. (2014) *GRL, 41*, 2738-2745. [6] Smith D.E. et al. (2010) *Space Sci. Rev. 150*, 209-241. [7] Lemelin M. et al. (2016) *Icarus, 273*, 315-328. [8] Matsunaga T. et al. (2001) *Proc. SPIE, 4151*, 32-39. [9] Haruyama J. et al. (2008) *EPS, 60*, 243-255. [10] Yokota Y. et al. (2011) *Icarus, 215*, 639-660. [11] Lucey P.G. et al. (2000) *JGR, 105*(E8), 20,297-20,305. [12] Lawrence D.J. et al. (2002) *JGR, 107(E12)*, 5130. [13] Hapke B. (2001) *JGR, 106(E5)*, 10,039-10,073. [14] Lucey P.G. and Riner M.A. (2011) *Icarus, 212*, 451-462. [15] Pieters C.M. et al. (1993) *JGR, 98(E11)*, 20,817-20,824. [16] Lucey P.G. (1998) *JGR, 103(E1)*, 1703-1713.